Institute of Paper Science and Technology
Atlanta, Georgia

IPST TECHNICAL PAPER SERIES

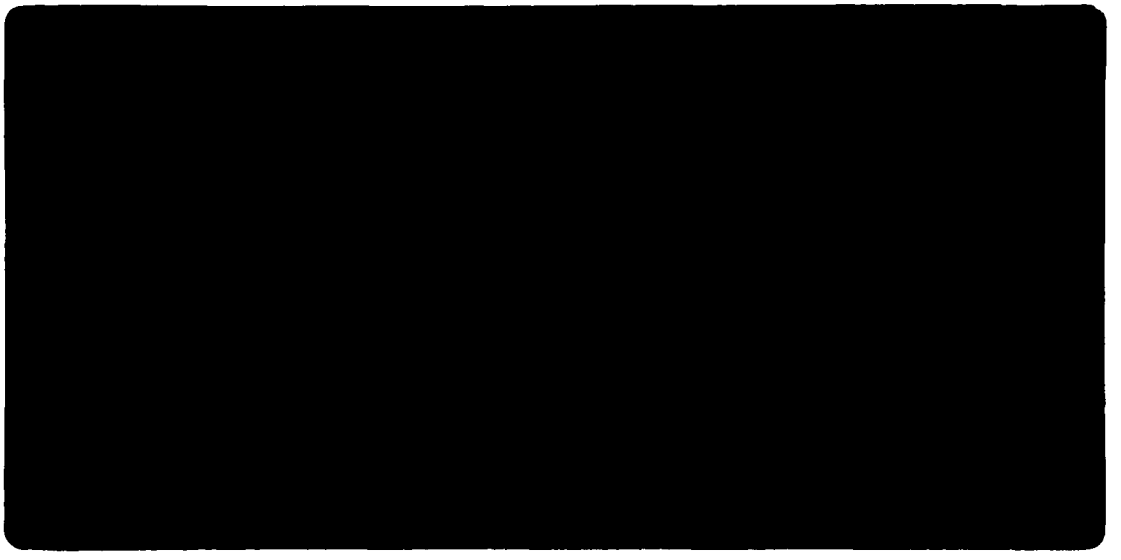

NUMBER 422

A TECHNIQUE FOR ANALYSIS OF GLOBALLY UNSTABLE FLOWS: APPLICATION TO A COATING SYSTEM

C.K. AIDUN

FEBRUARY 1992

A Technique for Analysis of Globally Unstable Flows: Application to a Coating System

C.K. Aidun

To be submitted to
J. Fluid Mechanics

A Technique for Analysis of Globally Unstable Flows: Application to a Coating System

Cyrus K. Aidun

Engineering Division
Institute of Paper Science and Technology
Atlanta, Georgia 30318

EXECUTIVE SUMMARY

This report outlines a formulation for the analysis of flow instability and transition to unsteady state in confined flow systems. As an example, it is applied to a lid-driven cavity simulating the pond of a short-dwell coater. This report was originally prepared and submitted to the National Science Foundation for time allocation on the Supercomputer Center. Since the report presents novel mathematical formulations for stability analysis of fluid flow systems in a number of relevant papermaking and coating processes, the author was encouraged to publish this information as an IPST Technical Report.

The formulation is generalized such that it applies to a broad class of fluid flow problems in the industry. In its current form, it applies only to geometries with regular boundaries that fit an appropriate orthogonal coordinate system. The equations can be modified for other irregular geometries.

The formulations are presented in abbreviated form; the lengthy derivations and proofs are not included in the paper. The author will be glad to share this information with interested individuals. The material in this report is being submitted for additional funding; we, therefore, request that the member companies do not share this information with individuals not affiliated with their company until it is published in the open literature.

I. INTRODUCTION

A. Outline

The mathematical technique presented in this report can be used to explore the stability properties of the shear-driven confined flow in a lid-driven cavity (LDC). This classical hydrodynamic system (Fig. 1) has been studied in the past for its simple geometry and boundary conditions. It provides an ideal system for a) examination and verification of numerical algorithms for solution of the Navier-Stokes equation; and b) analysis of a confined "stationary, captive" (Roshko, 1955) primary vortex, secondary corner vortices, as well as the appearance of Taylor-Görtler-like vortices (Koseff and Street, 1984) prior to transition to turbulence. Despite the tremendous popularity of this hydrodynamic system, its stability characteristics have remained virtually unexplored.

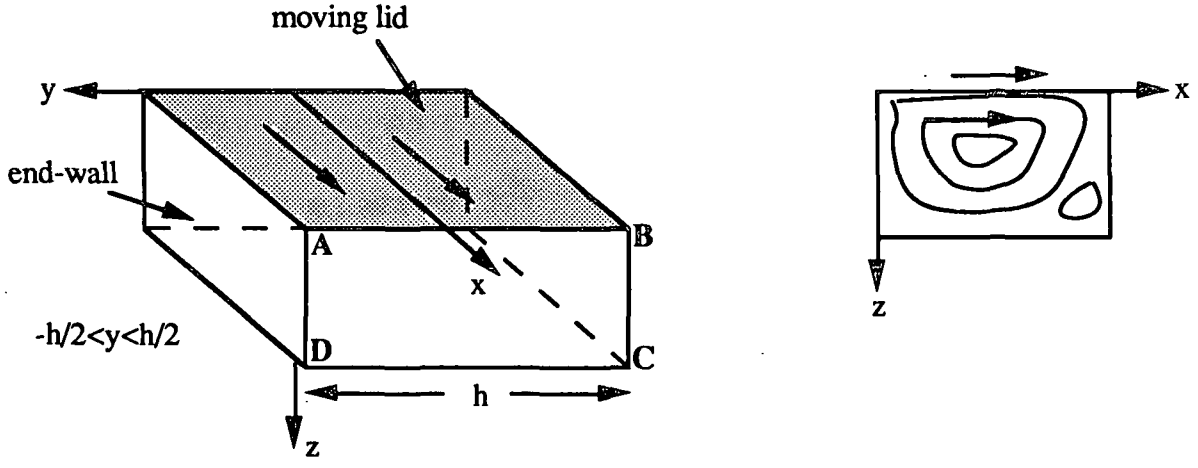

Fig. 1 Schematic of a lid-driven cavity.

In this research, we focus on the global stability properties of the primary steady state and its transition to time-periodic flow. The bifurcation diagram for the system will be constructed and the mutation of the steady states with the cavity span aspect ratio, h, will be investigated.

In addition to its fundamental importance as a classical hydrodynamic system, the lid-driven cavity is an idealized representation of a broad class of devices used in surface treatment and coating of paper, photographic films, and printing devices. In all of these applications, the desirable flow regime is the primary steady state which is almost two-dimensional (2-D). In fact, instability of this state and its transition to an unsteady or secondary multicellular steady state will result in operational difficulties (Aidun and

Triantafillopoulos, 1990). Therefore, the results from this research, in addition to providing a better understanding of the fundamental issues, offer a guideline and basis for the study and improvement of these and other technologically important manufacturing devices.

We shall solve for the steady state solution branches and pinpoint their bifurcation points using a global spectral method and a pseudoarclength continuation technique. Previous experimental studies (Aidun et al., 1990) show that, similar to the finite Taylor-Couette system, the LDC flow also exhibits multiple stable steady states. If these states are isolated in the phase space, then it will not be possible to detect and compute them from local bifurcation analysis of the primary branch. To resolve this, we shall take the following approach:

1) We will consider an *ideal*[1] LDC which is characterized by free-slip end walls. The 2-D steady-state solution branch representing the *primary*[2] branch for this ideal three-dimensional (3-D) system will be computed. The stability of the primary state will be examined by forming the linearized 3-D stability equations with the 2-D solution as the base state. In addition to the cavity Reynolds number, R, a second parameter, the span aspect ratio, h, will enter the stability analysis. Because of the free-slip end walls, the first bifurcation will be to a solution branch representing a 3-D cellular flow which is spatially periodic in the spanwise (y) direction. By computing the stability boundary for a 1-cell pattern, the entire stability boundary for $0<h<\infty$ will be determined using a simple mapping procedure explained by Aidun (1987).

2) We will extend the results for the ideal case to the real 3-D cavity flow (no-slip end walls) by applying Schaeffer's homotopy (Schaeffer, 1980) between the two flow systems. The homotopy parameter, $\tau = 0$, represents the ideal LDC (periodic) flow, where $\tau = 1$ represents the flow in a real LDC system.

The advantage of the stepwise approach outlined above is that it allows for a smooth decoupling of the *nongeneric* bifurcation diagram of the ideal LDC flow to the *generic* solution structure of the real system. This gives access to solution branches which emanate from the primary branch when $\tau = 0$, but decouple and become isolated when $\tau \neq 0$.

---

[1] We refer to a lid-driven cavity with free-slip end walls as an ideal LDC.

[2] A primary solution or state is one that forms at $R=0^+$.

In summary, we will compute the nongeneric (perfect) bifurcation diagram for the ideal LDC flow using a global spectral method with a pseudoarclength continuation technique. The bifurcation diagram will then be decoupled using a homotopy to perturb and gradually transform the ideal system to the real LDC flow. With this scheme, the state diagram of the 3-D cavity flow will be constructed revealing its global stability properties. Results from the proposed research will establish a frame of reference and a guideline for analysis of a large class of engineering and manufacturing devices that exhibit similar hydrodynamic characteristics.

B. Rationale and Objectives

The local and global stability of the primary steady-state flow in a driven cavity and its transition to a time-dependent state have remained unexplored despite their technological and fundamental significance. A driven cavity represents a simplified version of a class of surface treatment and coating devices used widely in the paper, photographic film, printing, and other industries. In these applications, the fluid (e.g., coating color, photosensitive chemicals, ink, lubrication oil) is applied uniformly on the surface of the substrate (e.g., paper, photographic film, printing plate, thrust bearings with grooves), which drives the flow inside the cavity.

As an example, Fig. 2 illustrates a coating head widely used for high-speed precision coating of paper. This device, known as a "short-dwell coater," is used to apply a thin uniform film on the surface of the substrate. As the roll speed increases beyond a critical limit, however, the film thickness becomes nonuniform and streaks develop in the machine direction (Fig. 3). Triantafillopoulos and Aidun (1990) showed that these streaks are caused by the instability of the roll-shaped primary state (Fig. 4a) and appearance of 3-D multicellular patterns (Fig. 4b) in the reservoir of these coaters. Recent experiments by Aidun et al. (1991) show that the primary steady state loses stability to finite-amplitude disturbances and competes with 3-D multicellular steady state flow patterns, similar to the one presented in Fig. 4b, before it becomes locally (linearly) unstable to a time-periodic state at R=800. Therefore, it is the global stability properties of the primary state that are of practical interest. These observations have motivated the proposed analysis for better understanding the global stability properties of the primary state, the ideal flow for these coating systems.

Similarly, the instability of the primary steady state in this device gives rise to "metering nonuniformities" when used in other applications such as size presses or Flexographic printing machines. Since problems of this kind cannot be tolerated in manufacturing, these instabilities impose an upper limit on the operational speed, and therefore production capacity, in the industry.

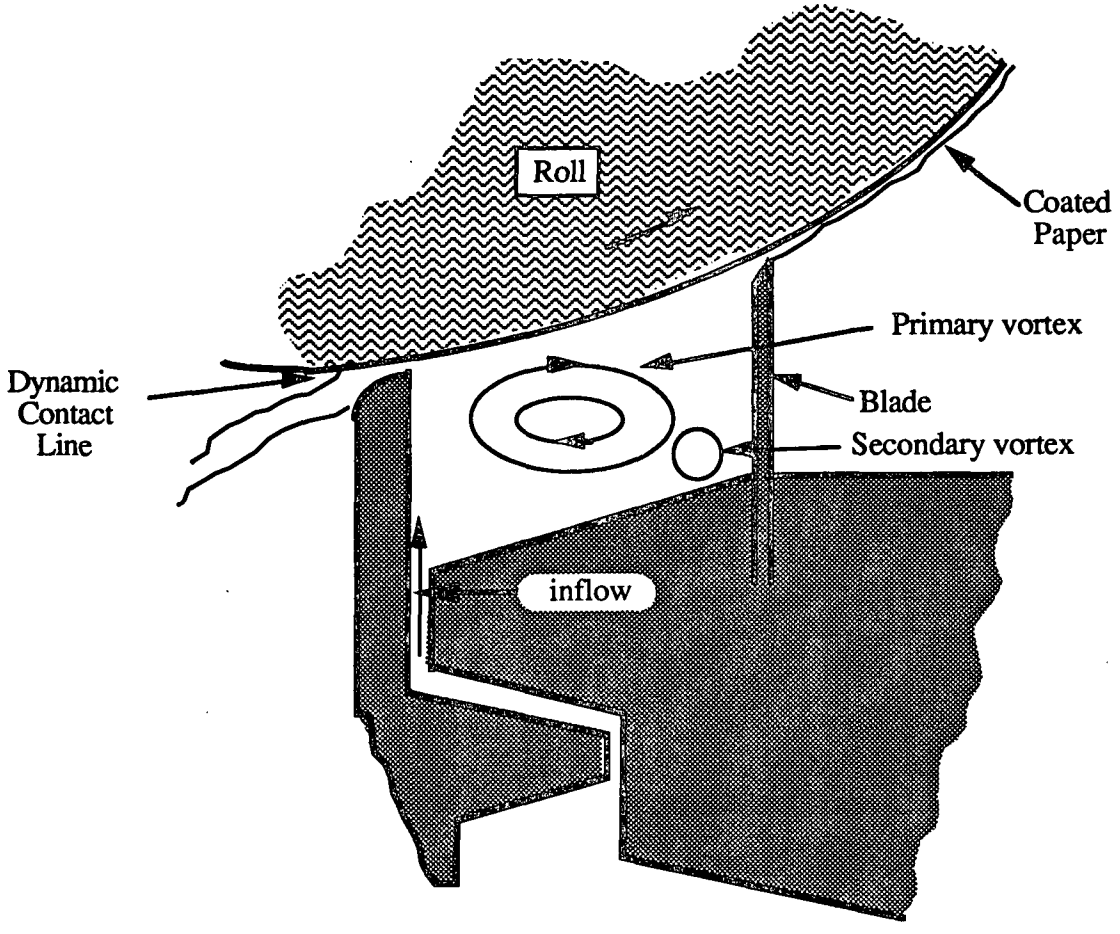

Fig. 2 Schematic of a short-dwell coater.

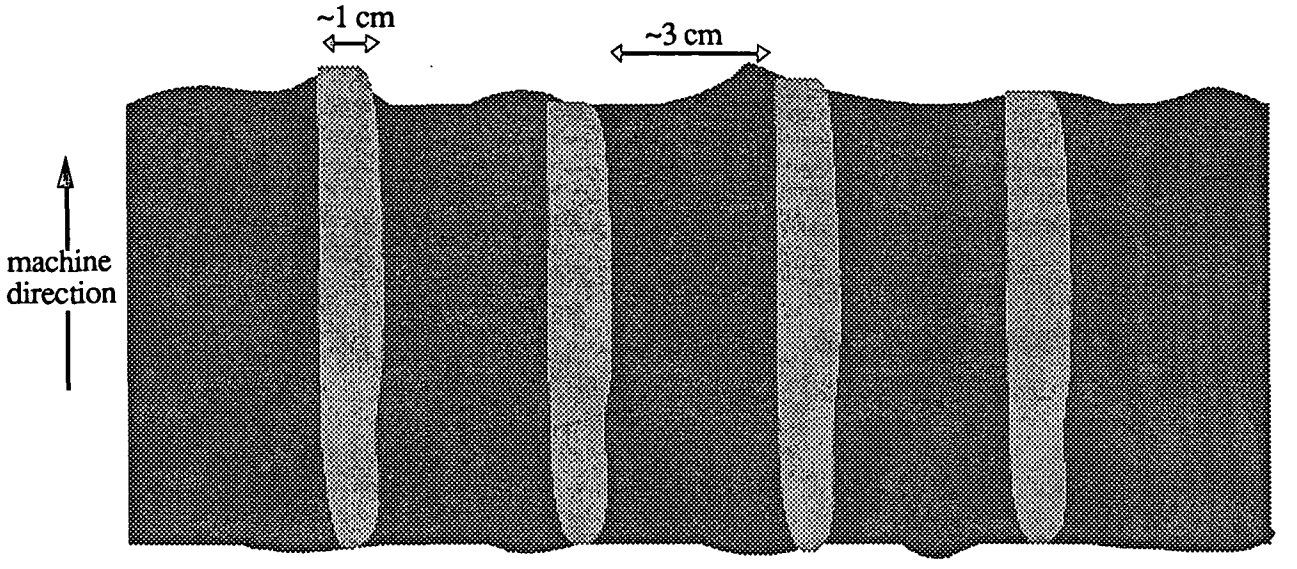

Fig. 3 Schematic of the streaks on paper coated with a short-dwell coater.

(a)

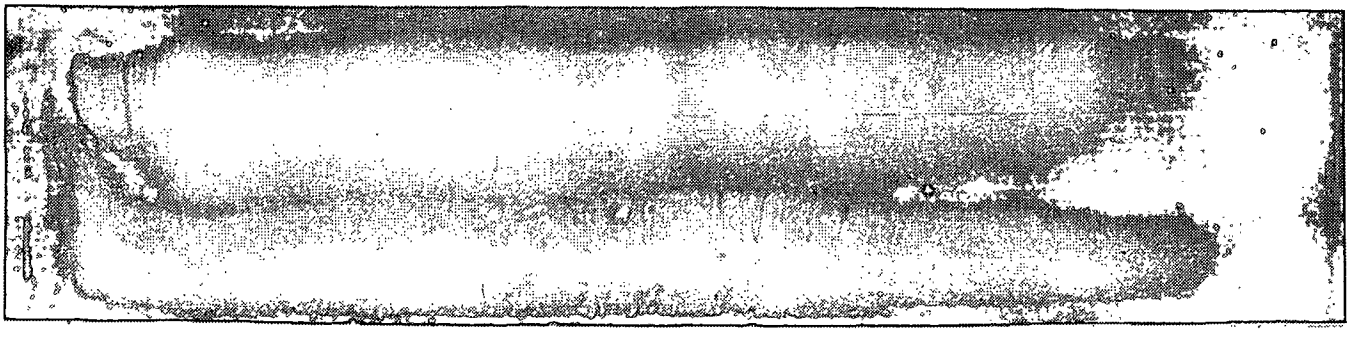

(b)

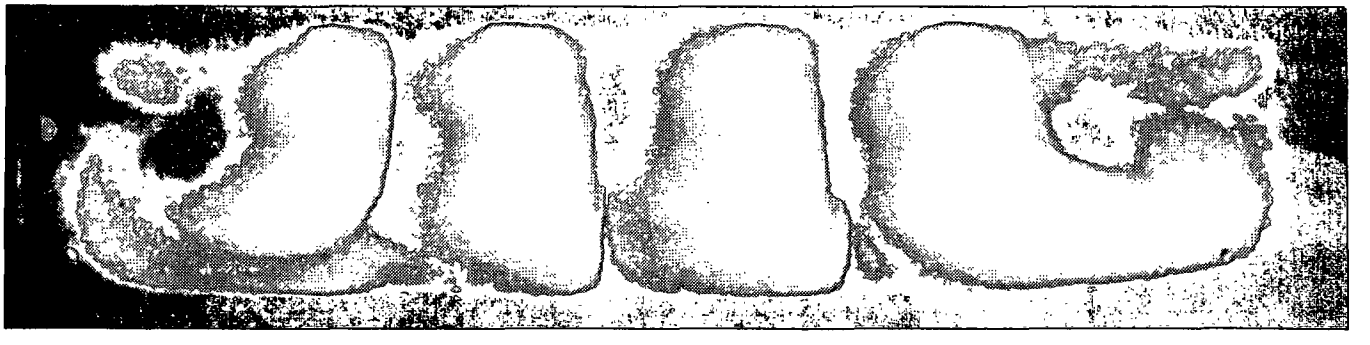

Fig. 4 Two competing steady states in a lid-driven cavity simulating the pond of a short-dwell coater; (a) primary steady state is almost 2-D and results in a uniform coating thickness (b) the 3-D multicellular steady state results in streaks illustrated in Fig. 3; both pictures are viewed from the ABCD plane of Fig. 1 (from Aidun et al., 1991).

It is extremely difficult and inefficient to analyze the stability characteristics of these complicated devices without knowing the stability properties of their ideal version represented by a LDC. The proposed research characterizes the fundamental aspects of the flow behavior in a driven cavity and provides a basis upon which these technologically important systems can be analyzed.

In addition to these practical considerations, several fundamental issues shall be investigated in this project. Amon and Patera (1989) demonstrated that, in general, the bifurcation in the initial transition process has a critical role in the transition to turbulence. In plane Poiseuille flow, a subcritical primary bifurcation gives rise to a broad band secondary instability and consequently an abrupt transition, while a supercritical primary bifurcation in Taylor-Couette-like systems results in a very different narrow band transition near criticality. By pinpointing the first transition of the primary state to a time-dependent state and analyzing the destabilizing disturbance structure, the initial dynamics leading the system en route to turbulence will be determined.

The objectives of this research are twofold: 1) to determine the global stability of the primary state by computing the critical Reynolds number for the onset of secondary locally stable states competing with the primary solution; this involves construction of a homotopy between the spatially periodic solution of the ideal LDC and the real system as described in Section D, and 2) to compute the primary steady state branch up to the transition to time-dependent flow and to construct the destabilizing disturbance structure and subsequently determine the physical mechanism responsible for the transition to time-periodic flow; specifically, to determine whether the primary bifurcation is due to the instability of the concave shear layer formed between the primary and the downstream secondary eddies (Görtler instability) or is caused by the centrifugal instability of the individual eddies (Taylor instability).

C. Background

The two-dimensional LDC flow was initially studied in detail by Burggraf (1966) who solved the two-dimensional Navier-Stokes equations for R=0 to 400. Pan and Acrivos (1967) used this system to examine Prandtl (1904) and Batchelor's (1956) theorem regarding the inviscid core that forms in a flow with closed streamlines surrounded by a thin shear layer at the boundary at high Reynolds number. They conclude that in the limit

as R-->∞, the flow in a LDC with a finite aspect ratio consists of a single inviscid core of uniform vorticity with an infinitesimally thin viscous layer along the solid boundary. The two-dimensional cavity flow has been computed accurately for large Reynolds numbers by several investigators (for example see Ghia et al., 1982). These studies, however, do not consider the three-dimensional features of this system.

In a series of informative experiments, Koseff and Street (1984) studied the three-dimensional aspects of flow in a cavity. In their experiments, the flow starts impulsively by a sudden acceleration of the top surface to speeds corresponding to the cavity Reynolds number ranging from 1000 to 10000. Their flow visualization studies reveal several interesting features including the appearance of local Taylor cells during the initial transients and the Taylor-Görtler-like (TGL) vortices. Kim and Moin (1985) captured these TGL vortices by numerically solving for the flow in an ideal LDC (free-slip end walls) at R=1000. A number of other three-dimensional numerical simulations solve the cavity flow at higher R values. For example, Freitas and Street (1988) and Perng and Street (1989) consider a cavity with span:depth:width aspect ratio 3:1:1 at R=3200. At this Reynolds number they show the dynamics of unsteady TGL vortices. Iwatsu et al. (1989) computed a 3-D steady flow at R=2000 and unsteady flow at R=3000 for a cubic cavity giving a range for the critical R.

Our flow visualization studies (Aidun et al., 1991) of a LDC (aspect ratio 3:1:1) with a small amount of through-flow show that a) the primary steady state becomes linearly unstable to a time-periodic flow at R=800, and b) the primary steady state becomes globally unstable and competes with at least three other secondary steady states with multicellular flow patterns before it destabilizes locally. These experiments show that the magnitude of the mass flow rate through the cavity does not change the qualitative behavior of the multiple stable states. Based on these observations, we have suggested that the primary steady state in a confined LDC also becomes globally unstable at a finite Reynolds number before destabilizing locally. Furthermore, we have suggested that the secondary steady states, similar to the Taylor-Couette system, are the decoupled secondary supercritical bifurcation branches of the ideal LDC (see Fig. 5). In this research project, we rigorously examines these conjectures.

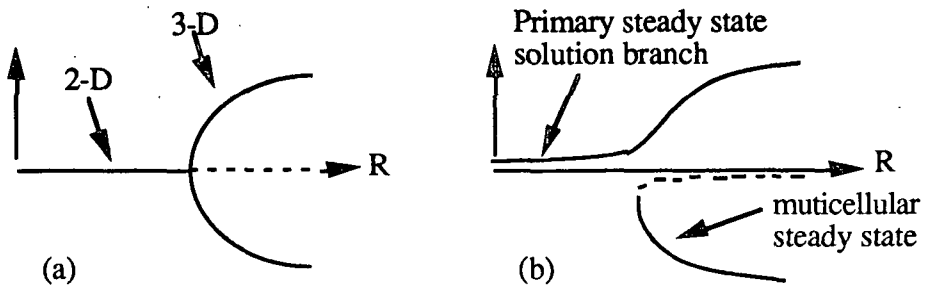

Fig. 5 Illustration of the decoupling of a perfect bifurcation (a) for an ideal LDC to a generic solution structure (b) for a real LDC.

D. Formulation

The tasks in this research project are: 1) to compute the critical Reynolds number as a function of the span aspect ratio for local stability of the 2-D steady state flow to 3-D disturbances in an ideal LDC with periodic or free-slip boundary conditions at the end walls, 2) to perturb the ideal system and decouple the spatially periodic solution branches to obtain the potentially isolated secondary steady state in a real LDC with a homotopy parameter, τ, ranging from 0 (ideal) to 1 (real); and 3) to trace the primary branch up to the first bifurcation point (which we have shown experimentally to be a time-periodic flow) and construct the destabilizing disturbance structure; this will determine the physical mechanism responsible for the initial transition, which leads the system to turbulence through a sequence of higher order transitions.

From the first two tasks of the proposed research, we shall determine the local as well as global stability properties of the steady state flow by constructing the perfect and imperfect bifurcation diagrams of the ideal and real systems, respectively. In previous computational analyses of the LDC, an initial-value problem is solved via finite-difference, finite-element, or pseudospectral methods. Recent experiments (Aidun et al., 1991) suggest the existence of multi-stable steady state solution branches which may be isolated from the primary state. The limited three-dimensional solutions available do not provide information regarding the stability of the flow. In contrast to the previous studies, the proposed research solves the governing equations as a bifurcation problem with the Reynolds number, the span aspect ratio, and the homotopy factor as the relevant parameters.

The final task provides a better understanding of the primary transition leading the system to turbulent flow. The physics of this instability is yet unresolved.

There are at least two mechanisms by which the 2-D primary steady state in a cavity with infinite span can destabilize and be replaced by a steady spatially periodic 3-D state. The first mechanism involves the Görtler-type instability of the concave viscous layer that forms between the primary and the downstream secondary eddies. The Taylor-Görtler-like vortices observed in the unsteady regime are attributed to this mechanism (Koseff & Street, 1984). In contrast to the Görtler vortices, which appear in a concave boundary layer having a length scale in the order of the boundary layer thickness (Peerhossaini and Wesfreid, 1988), the TGL vortices observed experimentally by Koseff & Street (1984) and computed numerically by a number of investigators (Freitas and Street, 1988; Perng and Street, 1989; Iwatsu et al., 1989), occupy the whole region of the downstream secondary eddy. It has yet to be established whether the concave viscous layer instability between the primary and the downstream secondary eddies or a different mechanism gives rise to these vortices. Flow visualization experiments (Aidun et al., 1991) show that at onset of the time-periodic state, a weak toroidal vortex superimposes on the downstream secondary eddy. This could be caused by Taylor-type centrifugal instability of the secondary eddy. The proposed decomposition and construction of the destabilizing disturbance structure will result in understanding the physical mechanism of this transition.

The solution procedure is similar to Steen and Aidun's (1988) analysis of Rayleigh-Benard-like convection in porous media. The dependent variables are projected onto a set of orthogonal basis functions; using Galerkin's method, the governing equations are reduced to a set of ordinary differential equations (ODE). The ODE system is treated as a bifurcation problem, and an arclength continuation technique is used to trace the solution branches to the point of bifurcation. In contrast to the convection-in-porous-media problem, where the governing equations can be reduced to a single scalar integrodifferential equation (Steen, 1986), the full Navier-Stokes (N-S) equation has to be solved for the problem at hand. This requires an efficient numerical scheme.

Our approach combines several new features with a global spectral expansion of the 3-D domain to increase its numerical efficiency and facilitate branch tracing and stability analysis. The first feature is the application of a divergence-free basis vector which inherently satisfies the continuity constraint and allows expansion of the three-dimensional velocity field in terms of only two scalar functions, eliminating one of the dependent variables (see Appendix A for details). Furthermore, the Galerkin method proposed in this research projects the governing equations on a set of divergence-free basis vectors,

explicitly eliminating the pressure terms from the momentum equations and thereby eliminating another dependent variable (Appendix A). The two components of the momentum equation are then expanded in terms of two scalar basis functions.

A unique feature of the LDC system is the discontinuity at the common edge of the moving lid and the stationary side walls. To remove this discontinuity, we reduce the velocity field, **v**, with respect to a basic flow field, **U**, which must satisfy the boundary conditions as well as the continuity equation. The reduced velocity field,

$$\mathbf{u} = \mathbf{v} - \mathbf{U} \tag{1}$$

then has homogeneous boundary conditions

$$\mathbf{u} = 0 \quad \text{on} \quad \partial\Omega \tag{2}$$

where $\partial\Omega$ is the entire boundary of the LDC. Using the 2-D Stokes flow for the basis velocity field is preferred since it preserves higher order regularity and also reduces the number of viscous terms in the final equation of motion, given by

$$\frac{\partial \mathbf{u}}{\partial t} + \mathbf{u}\cdot\nabla\mathbf{u} + \mathbf{u}\cdot\nabla\mathbf{U} + \mathbf{U}\cdot\nabla\mathbf{u} + \mathbf{U}\cdot\nabla\mathbf{U} = -\frac{1}{\rho}\nabla p' - \nu\nabla^2\mathbf{u} \ . \tag{3}$$

Here p' is the pressure reduced by the Stokes-flow pressure field, and the Stokes terms in the RHS have canceled each other. The reduced velocity field in the ideal system vanishes on the entire boundary, $\partial\Omega$, and the homogeneous boundary condition greatly simplifies the expansion of the dependent variables. However, the Stokes solution, **U**, and its derivatives appear explicitly in (3) and need to be evaluated. In contrast to the Rayleigh-Benard systems (Steen and Aidun, 1988) or the rotating disk-and-cylinder system (Hort, 1920; Chiao and Chang, 1990) where an analytical form of the basic flow solution is available, the LDC system's unique combination of geometry and boundary conditions, as Burggraf (1966) remarked, precludes an analytical Stokes solution. Analytical Stokes solutions exist only in asymptotic limits of infinitesimal height (Pan and Acrivos, 1967) and at corner regions (Moffatt, 1964), neither of which can be used in this analysis. A numerical solution of the Stokes flow by finite difference or finite element, although it can easily provide accurate results, is not an attractive option when considering the inaccuracy

and inefficiency of numerical differentiation and integration of the terms that appear in the equations. To resolve this difficulty, we have applied a Biharmonic Boundary Integral Formulation (BBIF) to this problem to solve the 2-D Stokes field in a series form (see Appendix B for details). This feature of our approach has several advantages. The series solution in terms of a small number of boundary nodes can be differentiated analytically with no loss of accuracy or addition of computational time. Also, this allows an analytical integration of the terms in the global spectral formulation containing **U** and its derivatives, eliminating a need for numerical differentiation or integrations altogether.

In summary, we shall expand the reduced velocity field in terms of a divergence-free basis vector

$$\mathbf{u} = \sum_{i=1}^{N} \alpha_i(t)\, \Phi_i(x) \qquad (4)$$

where $\nabla \cdot \Phi_i = 0$ in Ω
and $\Phi_i = 0$ on $\partial\Omega$.

Substituting this expansion into the reduced N-S equation (3) and applying Galerkin's method, we transform the equations of motion to a set of ODE given by

$$A_{ij}\, \dot{\alpha}_i = B_{ijk}\, \alpha_j\, \alpha_k + C_{ij}\, \alpha_j + D_i \qquad i = 1,..., N \qquad (5)$$

These coefficient matrices have several symmetry conditions which shall be used to optimize the computational procedure. Also, the combination of Chebyshev polynomials used to construct Φ_i is carefully selected to reduce the bandwidth of the coefficient matrices. The odd and even form of these basis functions decouples A_{ij} into four small independent partitions, which significantly reduces the computational time required for its solution.

We shall first investigate the stability of the primary steady state branch (2-D flow) in an ideal LDC (i.e., free-slip end walls). Here, the 2-D velocity components of the base flow are expanded by Chebyshev polynomials, and the third dimension, that is, the disturbance velocity component in the spanwise direction, is expanded in terms of Fourier series. Note that in this problem free-slip boundary conditions are identical to spatially periodic boundary conditions. We expect that, similar to a Taylor-Couette system, the first

bifurcating branch from the primary state will be a spatially periodic cellular structure. The stability boundary for this transition shall be computed using parametric continuation in the spanwise aspect ratio, h. The mapping procedure used by Aidun (1987) in the case of the Rayleigh-Benard convection in porous media will be applied here to determine the stability boundary in the range $0< h <\infty$.

The next step is the application of Schaeffer's (1980) homotopy to this problem. At the two end walls we prescribe a two-parameter family of boundary conditions with a homotopy parameter, τ, and the span aspect ratio, h. These are

$$\mathbf{v}\cdot\mathbf{n} = 0 \tag{6}$$

and

$$\tau\, \mathbf{v} + \frac{1}{h}(1-\tau)\, \mathbf{n} \circ \nabla \mathbf{v} = 0 \qquad \text{at the end walls.} \tag{7}$$

where, $\mathbf{v}$ is the velocity vector and $\mathbf{n}$ is unit vector normal to the end walls. A two-parameter family of solenoidal (divergence-free) basis functions, which inherently satisfies the boundary conditions (6) and (7), is constructed in Appendix C. Starting from the periodic steady solution of the ideal LDC, we shall compute the primary and secondary modes of the real LDC represented by the decoupled bifurcation branches (Fig. 5). Then we use this real LDC solution point on each branch to trace out the bifurcation diagram of the potentially multi-stable solution branches using a pseudoarclength continuation technique.

E. Relevance to Other Research

Burggraf (1966) and Pan and Acrivos (1967) chose a lid-driven cavity system to examine the behavior of a confined recirculating flow. The two-dimensional driven cavity flow is considered in many other investigations, including numerous computational simulations which treat the system as a benchmark, to examine numerical algorithms. Koseff and Street (1984) were the first to extensively examine the three-dimensional driven cavity flow as it becomes turbulent at Reynolds number above 6000. Their work motivated a number of numerical studies (see Section C) which confirmed the appearance of Taylor-Görtler-like vortices observed in their experiments. These vortices occur at high Reynolds number where the flow is already unsteady.

The stability properties of the equilibrium solutions (states) of this system have remained virtually unexplored, however. The proposed research investigates the stability properties of the steady state flow in this system.

Previous computational studies solve an initial-value problem, and march in time to asymptotically approach an equilibrium solution. These studies have not examined the stability of their solution to finite-amplitude disturbances. Our experiments (Aidun et al., 1991) suggest that at some range of Reynolds number, multiple locally stable steady states coexist. The proposed global spectral technique with the pseudoarclength continuation of the equilibrium solutions and the decoupling of the perfect bifurcation system using Schaeffer's homotopy make it possible to examine the global stability characteristics of the LDC steady state flows.

It is shown (Koseff and Street, 1984, and Prasad and Koseff, 1989) that existence of the Taylor-Görtler-like vortices is important in generating turbulence. The appearance of these vortices is attributed to the instability of the viscous layer between the primary and downstream secondary eddies. Our study will rigorously examine this conjecture through construction of the destabilizing disturbance structure at the onset of time-periodic flow. This scheme has proved to be very effective in detecting the secondary traveling waves responsible for the transition to time-periodic flow in a Rayleigh-Benard system (see Steen and Aidun, 1988).

Appendix A

The velocity vector **u** of an incompressible flow can be written in terms of two scalar functions [Chandrasekar (1981)]

$$\mathbf{u} = \nabla \times (\psi \mathbf{i}) + \nabla \times (\Gamma \mathbf{j}) \tag{A1}$$

where **i** and **j** are the unit vectors in the x- and y-directions, respectively (see Fig. 1). In matrix form, (A1) reduces to

$$\mathbf{u} = \begin{bmatrix} u \\ v \\ w \end{bmatrix} = \begin{bmatrix} 0 \\ \psi_z \\ -\psi \end{bmatrix} + \begin{bmatrix} -\Gamma_z \\ 0 \\ \Gamma_x \end{bmatrix} \tag{A2}$$

Therefore, a divergence-free function, such as the basis function in (4), can be decomposed as

$$\{\Phi_i\} = \{\psi_i\} \oplus \{\Gamma_i\} \tag{A3}$$

This formulation inherently satisfies the continuity equation and eliminates one of the dependent variables. If the function $\mathbf{u}$ satisfies homogeneous boundary conditions, then (A1), as shown first by Leonard and Wray (1982), has the further advantage of explicitly eliminating the pressure term from the governing equations.

$$\int_{\Omega} \nabla p' \cdot \Phi_i = \int_{\partial\Omega} p' \, \Phi_i \cdot \mathbf{n} - \int_{\Omega} p' \, (\nabla \cdot \Phi_i) = 0 \tag{A4}$$

Here p' is the pressure reduced by the Stokes flow pressure field, and the divergence-free basic function Φ_i expands the reduced velocity vector **u** as shown by Eq. (4).

Appendix B

The biharmonic equation describing Stokes flow in a two-dimensional region Ω can be written in terms of the stream function, Ψ, and vorticity, ω, as

$$\nabla^2 \Psi = \omega \text{ and } \nabla^2 \omega = 0 \quad \text{on } \Omega \tag{B1}$$

Invoking Green's theorem, the solution to (B1) can be written in the standard boundary integral form as

$$\eta(p)\,\Psi(p) = \int_{\partial\Omega} \mathbf{n} \circ [\Psi(q)\nabla G_1(p,q) - G_1(p,q)\nabla\Psi(q)]\,d\sigma(q)$$

$$+\frac{1}{4}\int_{\partial\Omega} \mathbf{n} \circ [\omega(q)\nabla G_2(p,q) - G_2(p,q)\nabla\phi(q)]\,d\sigma(q)$$

$$\eta(p)\,\omega(p) = \int_{\partial\Omega} \mathbf{n} \circ [\omega(q)\nabla G_1(p,q) - G_1(p,q)\nabla\omega(q)]\,d\sigma(q)$$

$$p \in \Omega + \partial\Omega, \quad q \in \partial\Omega. \tag{B2}$$

Here, $\mathbf{n}$ is a unit vector normal to the domain boundary, $\partial\Omega$, and η is a geometric factor given by

$$\eta(p) = \begin{cases} 0 & , \quad p \notin \Omega + \partial\Omega \\ \dfrac{\alpha}{2\pi} & , \quad p \in \partial\Omega \\ 1 & , \quad p \in \Omega. \end{cases} \tag{B3}$$

The principal part of Green's function, G_1, and the second fundamental function, G_2, are given by

$$G_1 = \frac{1}{2\pi}\log|p-q| \tag{B4a}$$

$$G_2 = \frac{|p-q|^2}{2\pi}\left[\log|p-q| - 1\right]. \tag{B4b}$$

Discretizing the boundary and assuming piecewise constant function, the solution for Ψ and ω in (B2) can be represented in discretized form by

$$\mathbf{A}\,\underset{\sim}{\Psi} + \mathbf{B}\,\underset{\sim}{\Psi}_n + \mathbf{C}\underset{\sim}{\omega} + \mathbf{D}\underset{\sim}{\omega}_n = 0 \tag{B5a}$$

$$\mathbf{A}\underset{\sim}{\omega} + \mathbf{B}\underset{\sim}{\omega}_n = 0 \tag{B5b}$$

where $\underset{\sim}{\Psi}_n = n \bullet \nabla\underset{\sim}{\Psi}$; and $\underset{\sim}{\Psi}$, $\underset{\sim}{\Psi}_n$, $\underset{\sim}{\omega}$, and $\underset{\sim}{\omega}_n$ are the vectorized representation of Ψ, Ψ_n, ω, and ω_n values evaluated on the discretized boundary. The coefficient matrices, **A, B, C,** and **D** are defined by

$$A_{ij} = \int_{q\in\partial\Omega_j} \mathbf{n} \circ \nabla \log|q_i - q|\, d\sigma(q) - \eta_j d_{ij} \tag{B6a}$$

$$B_{ij} = -\int_{q\in\Omega_j} \log|q_i - q|\, d\sigma(q) \tag{B6b}$$

$$C_{ij} = \frac{1}{4}\int_{q\in\partial\Omega_j} \mathbf{n} \bullet \nabla\left\{|q_i - q|^2 \log|q_i - q| - |q_i - q|^2\right\} d\sigma(q) \tag{B6c}$$

$$D_{ij} = -\frac{1}{4}\int_{q\in\partial\Omega_j} \left\{|q_i - q|^2 \log|q_i - q| - |q_i - q|^2\right\} d\sigma(q) \tag{B6d}$$

where $\partial\Omega_j$ is the boundary increment between j and j + 1 and node i is at the midpoint of $\partial\Omega_i$. Two boundary conditions, $\underset{\sim}{\Psi}$ and $\underset{\sim}{\Psi}_n$, are used with (B5) to evaluate the other two dependent variables ($\underset{\sim}{\omega}$ and $\underset{\sim}{\omega}_n$) on the boundary. Then (B5) is used again to compute the dependent variables in Ω.

An advantage of this formulation is that the boundary discretization results in an analytical expression for the coefficient matrices and their derivatives. Furthermore, an analytical

solution of the integrals in (B6) is available (Jawson and Symm, 1977; and Kelmanson, 1982) and the singularities arising when $q \rightarrow q_i$ can be removed by application of Cauchy's principal value theorem. The above formulation, therefore, completely eliminates a need for numerical differentiation or integration and provides an efficient method for accurate evaluation of the Stokes velocity field and its derivatives in the global spectral equations.

Appendix C

The x-component of the boundary condition (7) is

$$\tau u + \frac{1}{h}(1-\tau)\, u_y = 0 \qquad \text{at} \qquad y = \pm h/2 \tag{C1}$$

where $u_y \equiv \frac{\partial u}{\partial y}$. Expanding u in terms of u_j, the x-component of basis function Φ_j, and substituting in (C1) we get:

$$\tau\, u_j + \frac{1}{h}(1 - \tau)\, u_{j,y} = 0 \qquad \text{at} \qquad y = \pm h/2 \tag{C2}$$

The basis function u_j can be written as:

$$u_j = F_l\,(x)\, G_m\,(z)\; H_n\,(y) \tag{C3}$$

where F, G, and H are functions of x, z, and y, respectively.

Substituting (C3) in (C2), we get:

$$\tau\, H_n\,(y) + \frac{1}{h}(1-\tau)\, H'_n\,(y) = 0 \qquad \text{at} \qquad y = \pm h/2 \tag{C4}$$

This boundary condition is satisfied if:

$$H_n\,(y) = T_{n+1}\,(y) - T_1\,(y) + \delta_n \operatorname{Cos}(n\pi y) \tag{C5}$$

$$\text{where } \delta_n = -\frac{1-\tau}{\tau} \quad \frac{(-1)^n}{h}\left[(2n+1)^2 - 1\right], \tag{C6}$$

T_n is the Chebyshev polynomial of degree n.

Functions F and G are constructed using Chebyshev polynomials such that they satisfy the no-slip boundary conditions and minimize the bandwidths of matrices in Eq. 5. When τ = 0, (C4) represents a free-slip boundary condition (or a periodic boundary condition in the

y-axis) and therefore (C3) expands the velocity field of an ideal LDC flow (or a LDC with infinite span). The base state for this case is simply the 2-D flow solution, which is easy to obtain. Since the coefficients in (3) have no dependence on y, the first critical mode that destabilizes the 2-D base state is periodic in y. The spatially periodic branch is then computed using continuation techniques. We then use τ as a small parameter to perturb the ideal case and obtain the decoupled bifurcation diagram. In the case of a Taylor-Couette system, Bolstad and Keller (1987) showed that the bifurcation diagram for small τ is qualitatively the same as that for τ=1.

The main advantage of this technique is that it allows detection and tracing of solution branches not connected to the primary branch and otherwise inaccessible.

ACKNOWLEDGEMENT

This research is a part of the IPST Project, Fundamentals of Coating Systems. This project is being funded in part by the member companies of the Institute, TAPPI Foundation Inc., and the National Science Foundation's Supercomputer Center. The author is grateful to the IPST Engineering Division Director, Dr. Richard Ellis, who has encouraged him to pursue and publish this work.

BIBLIOGRAPHY

Aidun, C.K., and Triantafillopoulos, N.G. 1990 *International Symp. Mech. Thin-Film Coating*, AIChE Spring Meeting, paper 96d.

Aidun, C.K., Triantafillopoulos, N.G., and Benson, J. 1991 *Phys. Fluid* **A 3** (9), 2081.

Aidun, C.K. 1987 *Bifurcation Phenomena in Thermal Processes and Convection.* HTD-Vol. **94** and AMD-Vol. **89**, 31.

Amon, C.H., and Patera, A.T. 1989 *Phys. Fluids* **A, 1**, 2006.

Batchelor, G.K. 1956 *J. Fluid Mech.*, **1**, 177.

Burggraf, O.R. 1966 *J. Fluid Mech.*, **24**, 113.

Chandrasekar, S. 1981 Hydrodynamic and Hydromagnetic Stability, Dover Publications, New York.

Chiao, S-M. F., and Chang, H-C. 1990 *J. Non-Newtonian Fluid Mech.*, **36**, 361.

Freitas, C.J., and Street, R.L. 1988 *Int. J. Num. Methods Fluid*, **8**, 769.

Ghia, U., Ghia, K.N., and Shin, C.T. 1982 *J. Comp. Phys.*, **48**, 387.

Hort, W.Z. 1920 Z. *Tech. Phys.* **10**, 213.

Iwatsu, R., Ishii, K., Kawamura, T., Kuwahara, K., and Hyun, J.M. 1989 *Fluid Dynamics Research*, **5**, 173.

Jaswon, M.A., and Symm, G.T. 1977 Integral Equation Methods in Potential Theory and Elastostatics, Academic Press, New York.

Karniadakis, G.E., Mikic, B.B., and Patera, A.T. 1988 *J. Fluid Mech.*, **192**,365.

Kelmanson, M.A. 1983 *J. Comp. Phys.*, **51**, 139.

Kim, J., and Moin, P. 1985 *J. Comp. Phys.*, **59** (2), 308.

Koseff, J.R., and Street, R.L. 1984 *J. Fluids Eng.*, **106**, 21(a) 385(b) 390(c).

Leonard, A., and Wray, A. 1982 NASA 7M-842267.

Moffatt, H. K. 1964 *J. Fluid Mech.*, **18**, 1.

Pan, F., and Acrivos, A. 1967 *J. Fluid Mech.*, **28**, 643.

Peerhossaini, H., and Wesfreid, J.E. 1988 In Propagation in Systems Far From Equilibrium, Springer-Verlag, New York.

Perng, C-Y, and Street, R.L. 1989 *Int. J. Num. Methods Fluid*, **9**, 341.

Prandtl, L. 1904 NACA Tech. Memo. 452.

Prasad, A.J., and Koseff, J.R. 1989 *Phys. Fluid* A, **1** (2), 208.

Roshko, A. 1955 NACA Tech. Note 3488.

Schaeffer, D. 1980 *Math. Proc. Cambridge Phil. Soc.*, **87**, 307.

Steen, P.H., and Aidun, C.K. 1988 *J. Fluid Mech.*, **196**, 263.

Steen, P.H. 1986 *Phys. Fluids*, **29**, 925.

Triantafillopoulos, N.G., and Aidun, C.K. 1990 TAPPI Coating Conference, also in*TAPPI J.*, **73** (6), 129.